AD/A-000 892

FEASIBILITY OF NEW LASERS

Lawrence H. Hall

Rocketdyne

Prepared for:

Army Missile Research, Development and Engineering Laboratory

8 November 1974

DISTRIBUTED BY:

NTIS

National Technical Information Service
U. S. DEPARTMENT OF COMMERCE
5285 Port Royal Road, Springfield Va. 22151

DISPOSITION INSTRUCTIONS

Destroy this report when it is no longer needed. Do not return it to the originator.

DISCLAIMER

The findings in this report are not to be construed as an official Department of the Army position unless so designated by other authorized documents.

TRADE NAMES

Use of trade names or manufacturers in this report does not constitute an official endorsement or approval of the use of such commercial hardware or software.

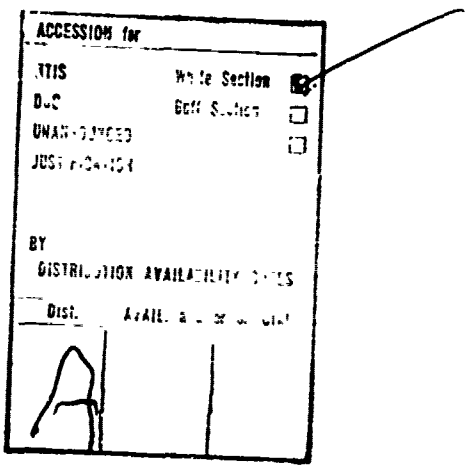

Unclassified

SECURITY CLASSIFICATION OF THIS PAGE (When Data Entered)

REPORT DOCUMENTATION PAGE		READ INSTRUCTIONS BEFORE COMPLETING FORM
1. REPORT NUMBER RK-CR-75-16	2 GOVT ACCESSION NO.	3 RECIPIENT'S CATALOG NUMBER AD/A-000 892
4. TITLE (and Subtitle) FEASIBILITY OF NEW LASERS		5 TYPE OF REPORT & PERIOD COVERED Final, 15 April 1974 through 26 September 1974
		6 PERFORMING ORG. REPORT NUMBER R-9597
7. AUTHOR(s) Lawrence H. Hall		8 CONTRACT OR GRANT NUMBER(s) DAAH-01-74-C-0586
9. PERFORMING ORGANIZATION NAME AND ADDRESS Rocketdyne Division, Rockwell International 6633 Canoga Avenue Canoga Park, California 91304		10 PROGRAM ELEMENT, PROJECT, TASK AREA & WORK UNIT NUMBERS
11. CONTROLLING OFFICE NAME AND ADDRESS Propulsion Directorate U.S. Army Missile Research, Development, Eng. Lab. U.S. Army Missile Command, Redstone Arsenal, Ala.		12 REPORT DATE 8 November 1974 13 NUMBER OF PAGES 68
14 MONITORING AGENCY NAME & ADDRESS(if different from Controlling Office)		15 SECURITY CLASS (of this report) Unclassified 15a. DECLASSIFICATION/DOWNGRADING SCHEDULE

16. DISTRIBUTION STATEMENT (of this Report)

Approved for Public Release;
Distribution Unlimited

17 DISTRIBUTION STATEMENT (of the abstract entered in Block 20, if different from Report)

18 SUPPLEMENTARY NOTES

Reproduced by
NATIONAL TECHNICAL
INFORMATION SERVICE
U S Department of Commerce
Springfield VA 22151

19 KEY WORDS (Continue on reverse side if necessary and identify by block number)

Lasers, chemical lasers, cesium, alkali metals, population inversions, alkali halides, chemiluminescence

20 ABSTRACT (Continue on reverse side if necessary and identify by block number)

Relative populations of alkali-metal atom excited states were determined spectroscopically for the Rb/Cl_2 and Cs/F_2 reaction systems at pressures near 1 torr. Several dozen population inversions were identified and measured for each. For the Cs/F_2 system a parametric study was performed on the effects of reactant ratios and pressures. Gain for the population inversions was estimated.

DD FORM 1 JAN 73 1473 EDITION OF 1 NOV 65 IS OBSOLETE

Unclassified

SECURITY CLASSIFICATION OF THIS PAGE (When Data Entered)

PREFACE

This report covers the period 15 April 1974 through 26 September 1974 and is the final report under Contract DAAH-01-74-C-0586. The cognizant project engineer monitoring the program is Dr. Barry Allan, U.S. Army Missile Command, Redstone Arsenal, Huntsville, Alabama.

The work reported here was carried out in the Laser Science and Engineering organization. The responsible engineer is Dr. L. H. Hall. Mr. J. Novak also contributed to the program.

CONTENTS

ILLUSTRATIONS

TABLES

INTRODUCTION AND SUMMARY

The objective of this study was to investigate selected alkali-metal halogen reactions to evaluate their potential for new chemical lasers at suitable wavelengths. Using techniques developed in the Discovery of New Lasers contract (DAAH01-73-C-0447), the chemiluminescence of the alkali-metal atoms was spectroscopically observed and was analyzed to measure population inversions in the excited electronic states of the alkali-metal atoms as a function of reaction conditions. The conditions included nozzle configuration, reactant ratios, and reactant pressures for the Cs/F_2 reaction system. Spatial scans were performed on one population inversion (5D-3/2→6P-3/2) and gains were calculated for all observed population inversions. Absorption and extinction experiments were also performed. For the Rb/Cl_2 reaction system fixed-point studies at 1 torr total pressures were performed.

For the Cs/F_2 reaction system more than three dozen population inversions were observed as a function of reaction conditions. It was calculated that 11 percent of the total reaction exothermicity is emitted by one set of transitions (5D→6P) exhibiting population inversion, and this energy may be available for lasing.

Calculated gains indicate a strong potential for lasing. An extinction measurement and a calculation indicates that CsF particulates will not prevent lasing.

Over a dozen population inversions were measured for the Rb/Cl_2 system. Because of the low exothermicity of this system, it is likely that inversions can be seen for Cs or Rb with other halogen-containing molecules such as NF_3, N_2F_4, ClF_3, or ClF_5 having similar low exothermicity reactions with alkali metals.

The results of this study have established the reaction conditions for the Cs/F_2 system most likely to give lasing.

TECHNICAL DISCUSSION

DESCRIPTION OF REACTION SYSTEM

For the general reaction of an alkali metal, M, with a halogen, X_2, the equations of reaction are

$$M + X_2 \longrightarrow MX(v) + X \qquad \text{Primary Reaction}$$

$$M_2 + X \longrightarrow MX(v) + M^* \qquad \text{Secondary Reaction}$$

$$MX(v) + M \longrightarrow MX + M^* \qquad \text{Transfer Reaction}$$

The exothermicities of the primary and secondary reactions are listed in Table 1 for several alkali-metal:halogen reaction pairs. The energies of the first excited state ($nP_{1/2}$) of the alkali-metal atoms are listed in Table 2. For either the primary or secondary reaction, the Cs/F_2 reaction pair is most exothermic. For a given halogen, the exothermicity decreases in the order--cesium, rubidium, potassium, sodium, lithium. For a given alkali metal, the exothermicity decreases in the order--fluorine, chlorine, bromine, iodine. In general, exothermicity is more responsive to a change in the halogen than to a change in the alkali metal. Some reactions lack the exothermicity to excite the first excited state ($nP_{1/2}$) of the alkali metal. For example, the primary reaction of the Na/Cl_2 system is exothermic by 35 kcal/mole, while the first excited state of Na lies at 48.5 kcal/mole, so (for this system) the primary reaction cannot be a significant pumping mechanism. For the Cs/F_2 system, both the primary and the secondary reactions produce enough energy to excite the Cs atom. It should be noted that the possibility does exist of an energy pooling reaction of the sort

$$MX(v') + MX(v'') \longrightarrow MX(v=o) + MX(v''')$$

TABLE 1. REACTION ENERGETICS

Alkali Metal	F_2	Cl_2
Cs	-85 $\frac{kcal}{mole}$	-49
	-112	-96
Rb	-78	-47
	-106	-95
K	-80	-44
	-106	-89
Na	-76	-35
	-96	-75

Heat of Reaction at 298 K

TABLE 2. ENERGIES OF FIRST EXCITED STATE ($nP_{\frac{1}{2}}$) AND IONIZATION ENERGIES FOR ALKALI-METAL ATOMS

	$nP_{\frac{1}{2}}$		First Ionization Energy	
Li	14,903 cm^{-1}	42.58 kcal	43,487 cm^{-1}	124.3 kcal
Na	16,956	48.45	41,449	118.4
K	12,98-	37.10	35,009	100.0
Rb	12,578	35.94	33,691	96.27
Cs	11,178	31.94	31,406	89.7[illegible]

where MX(v''') has sufficient energy to excite the alkali-metal atom while neither MX(v'') ncr MX(v') individually has sufficient energy.

The ionization energies of each of the alkali metals (Table 2) indicate that the secondary reaction of the Cs/F_2, Cs/Cl_2, and Rb/F_2 reaction systems all have sufficient energy to ionize the alkali-metal atom. Therefore, under certain experimental conditions, alkali-atom: electron recombination fluorescence might be seen.

As shown in Table 3, the dissociation energies of the alkali halide molecules are presented. All are quite stable except for perhaps RbCl whose dissociation energy is less than the exothermicity of the Rb/Cl_2 secondary reaction. Then RbCl might be unable to carry off the energy of the reaction and there is a possibility that direct excitation of the Rb atom would be strongly favored. Also, all rate constants would be affected.

TABLE 3. ALKALI HALIDE DISSOCIATION ENERGIES

	Cs	Rb	K	Na	Li
F	130kcal	120	$\leq$140	$\leq$120	$\leq$150
Cℓ	- -	>92.3	102	82.5	120
Br	$\geq$90	90	91.2	88.7	100
I	76	75.8	76.7	72.8	80

Some of the rate constants for the Na/Cl_2 reaction system have been measured by Polanyi and his co-workers, and individual rate constants for other systems have been measured using molecular beam techniques by Herschbach and his co-workers. All rates are quite fast (gas kinetic and, in some instances, faster due to a reaction cross section greater than the collision cross section). The rate constants for each reaction would not be expected to vary more than 30 to 40 percent depending on the alkali-metal:halogen system chosen.

REVIEW OF RELEVANT SPECTROSCOPIC DATA IN THE LITERATURE

Atoms

In Fig. 1 through 4 are shown the energy level diagrams for the alkali-metal atoms. The position of the states are generally well known and are tabulated in several places such as C. Moore's NBS Tables. These electronic levels are "one-electron" levels involving states of the outer s electron and resemble the H-atom levels. For the alkali-metal atoms, states involving promotion of an inner P electron lie at energies over 100,000 cm^{-1} and can be ignored. A number of sets of energy levels exist called S, P, D, F. G. etc., determined by the azimuthal quantum number $\ell = 0, 1, 2, 3, 4, 5, \cdots$. A selection rule exists such that only transitions for which

$$\Delta\ell = \pm 1$$

are allowed. Four sets of allowed transitions are given particular names:

Principal Series	ν = 1S - mP	m = 2,3...
Sharp Series	ν = 2P - mS	m = 2,3...
Diffuse Series	ν = 2P - mD	m = 3,4...
Fundamental Series	ν = 3D - mF	m = 4,5...

Each level is split into a doublet whose levels are designated by the quantum numbers $j = \ell + 1/2$ and $j = \ell - 1/2$. For the lowest P state of cesium, the splitting is 554 cm^{-1}. For each alkali metal, the doublet splitting decreases with increasing n and increasing ℓ. For the F and G states, the splitting is less than one wavenumber.

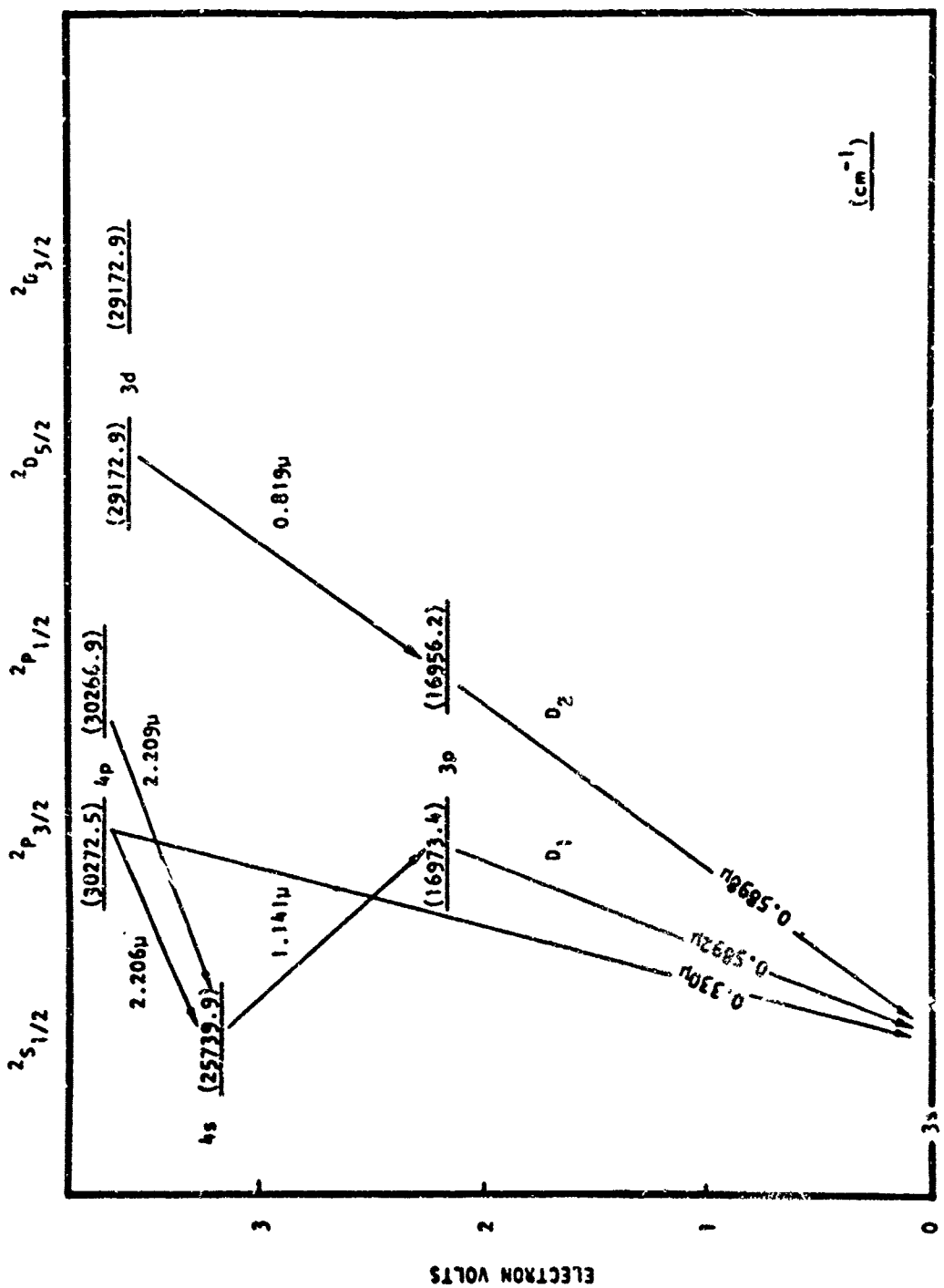

Figure 1. Low-Lying Energy Diagram of Atomic Sodium

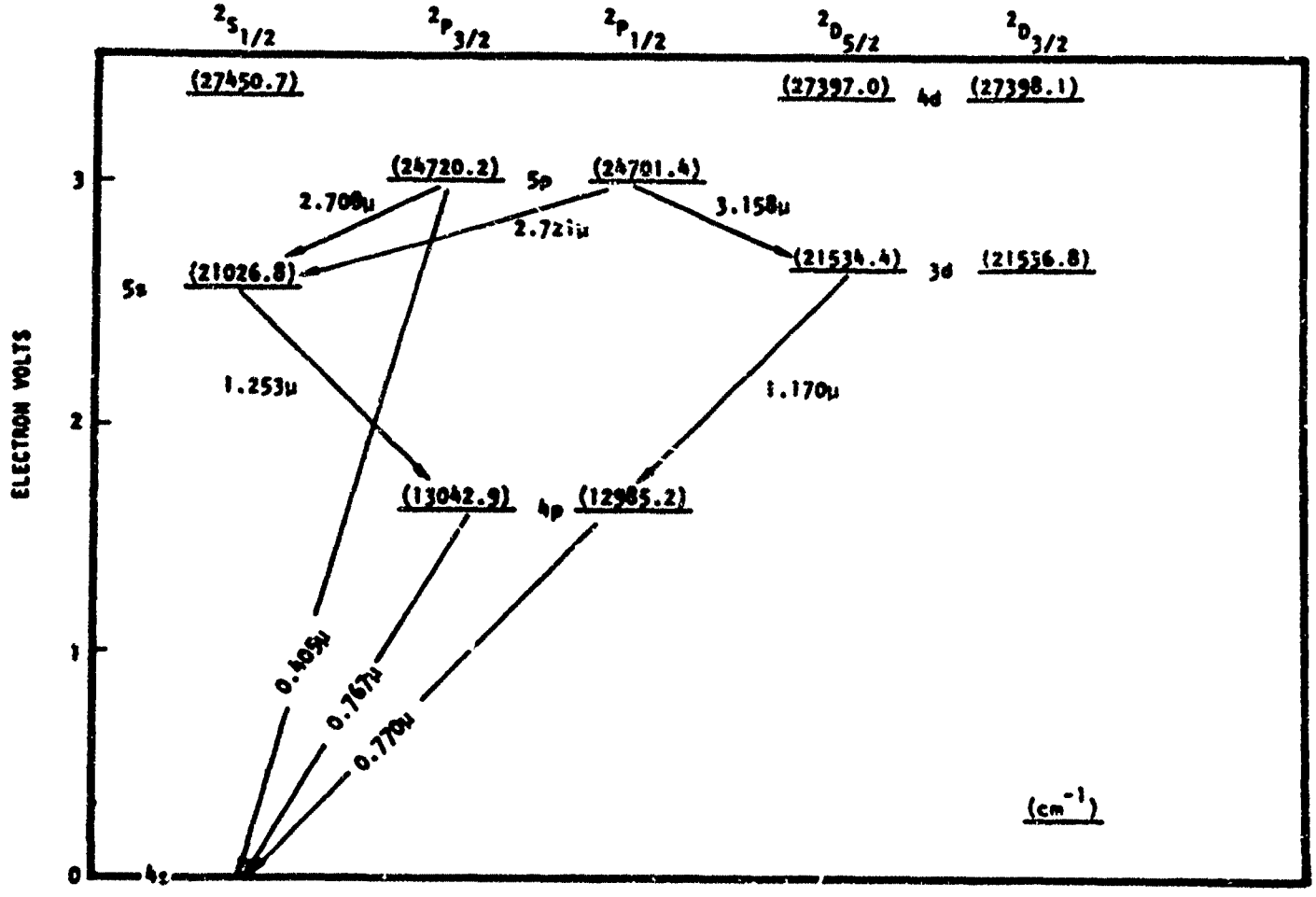

Figure 2. Low-Lying Energy Diagram of Atomic Potassium

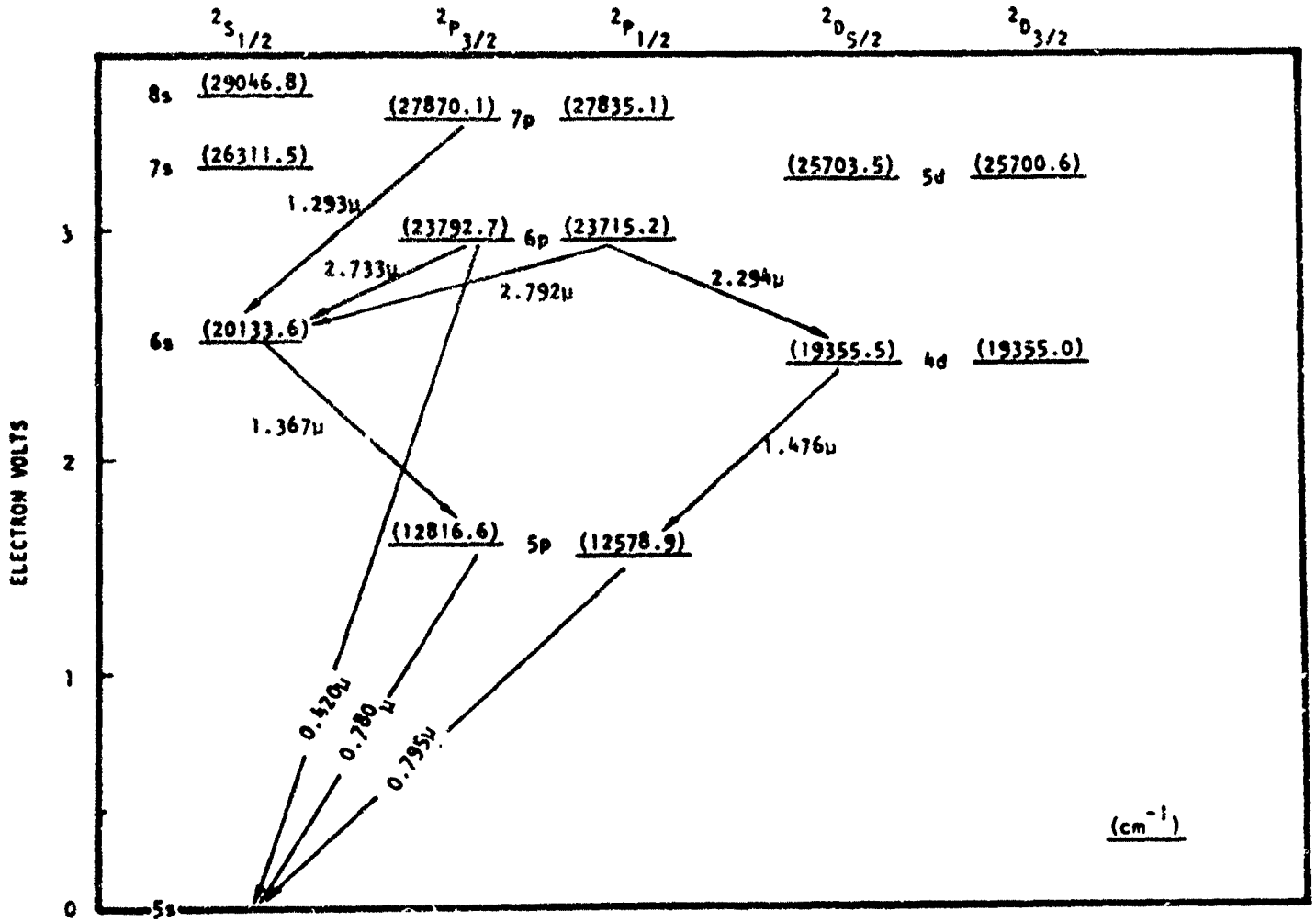

Figure 3. Low-Lying Energy Diagram of Atomic Rubidium

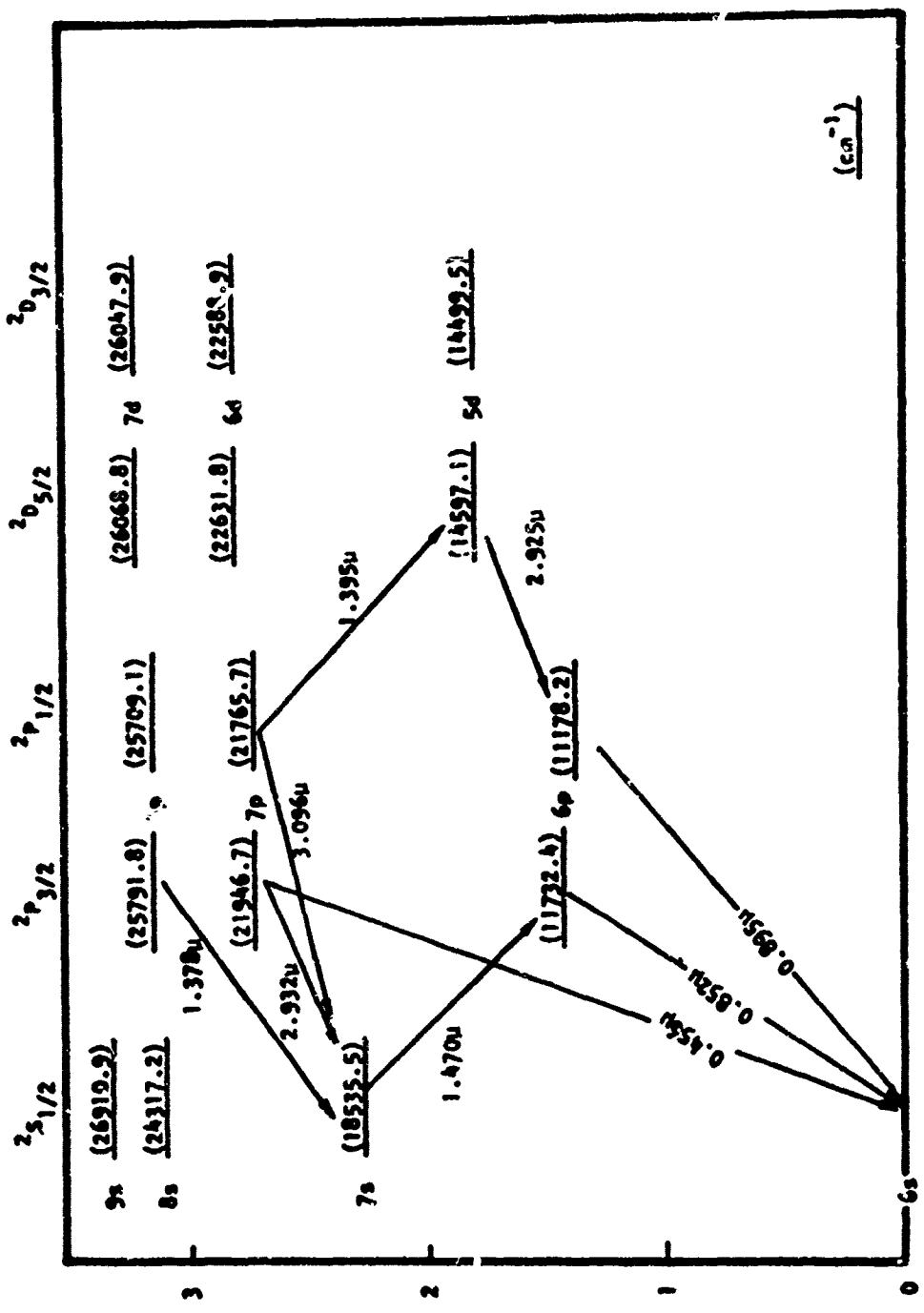

Figure 4. Low-Lying Energy Diagram of Atomic Cesium

In Table 4 the important radiative transitions are summarized. These transitions shift to the red with increasing atomic number, Z. In Table 5 the energies of some of the individual levels are listed. Not only does the energy above the round state of each level decrease with increasing atomic number, but the doublet splitting also increases. This latter effect is due to increased spin-orbit coupling. Table 6 presents a list of the first 44 energy levels for the cesium atom.

Some experimental data exist on the radiative transition probabilities of the lower states of Cs and Rb. A number of papers report on the transition probabilities of the principal series measured in absorption (Ref. 1 and 2). The transition probabilities for some of the other allowed transitions have been measured in high-temperature discharges, and some data exist on the transition probabilities for the forbidden S-to-D transitions.

A number of theoretical calculations of the transition probabilities of the alkali metals have been performed and the results are reported in the literature (Ref. 3 and 4). For transitions between the higher states, they are the only values available. The agreement between calculated and experimental values of radiative transition probabilities for transitions between the lower states is generally adequate. For higher states, the different calculations often show significant disagreement due to different treatment of spin-orbit coupling and the use of different wavefunctions.

In general, the literature on cesium is much more extensive than that on rubidium. A large body of literature exists on the properties of cesium plasma at high temperatures, including data on spectra and on linewidth.

TABLE 4. SUMMARY OF ELECTRONIC TRANSITIONS*

	n	$n+1\ ^2P_{3/2}$ / $n\ ^2S_{1/2}$	$n\ ^2P_{3/2}$ / $n\ ^2S_{1/2}$	$n\ ^2P_{1/2}$ / $n\ ^2S_{1/2}$	$n+2\ ^2P_{3/2}$ / $n+1\ ^2S_{1/2}$	$n+1\ ^2P_{1/2}$ / $n-1\ ^2D_{5/2}$	$n+1\ ^3S_{1/2}$ / $n\ ^2P_{3/2}$	$n-1\ ^2D_{5/2}$ / $n\ ^2P_{1/2}$	$n+1\ ^2P_{3/2}$ / $n+1\ ^2S_{1/2}$	$n+1\ ^2P_{1/2}$ / $n+1\ ^2S_{1/2}$
Cs	6	0.456	0.852	0.895	1.378	1.395	1.470	2.925	2.932	3.096
Rb	5	0.420	0.708	0.795	1.293	2.294	1.367	1.476	2.733	2.792
K	4	0.405	0.767	0.770	1.253	3.158	1.253	1.170	2.708	2.721
Na	3	0.330	0.5892	0.5898	1.075	9.150	1.141	0.819	2.206	2.209

*Units are Microns

TABLE 5. LIST OF LOW-ENERGY STATES OF THE ALKALI-METAL ATOMS

	n	n+1 S	n+2 S	n+3 S	n P 1/2	n P 3/2	n+1 P 1/2	n+1 P 3/2	n-1 D 3/2	n-1 D 5/2	n D 3/2	n D 5/2
Cs	6	18,535	24,317	26,910	11,178	11,732	21,765	21,946	14,499	14,597	22,588	22,631
Rb	5	20,133	26,311	29,046	12,578	12,816	23,715	23,792	19,355	19,355	25,700	25,703
K	4	21,026	27,450	30,274	12,985	13,042	23,701	24,720	21,534	21,536	27,397	27,398
Na	3	25,739	33,290	36,372	16,956	16,973	30,266	30,272	--	--	29,172	29,172
Li	2	27,206	35,012	38,299	14,903	14,904	30,925	30,925	--	--	--	--

TABLE 6. LIST OF ELECTRONIC STATES OF THE CESIUM ATOM

STATE	ENERGY
	$0 cm^{-1}$
6S-1/2	
6P-1/2	11178
6P-3/2	11732
5D-3/2	14499
5D-5/2	14597
7S-1/2	18536
7P-1/2	21766
7P-3/2	21947
6D-3/2	22589
6D-5/2	22632
8S-1/2	24317
4F	24472
8P-1/2	25709
8P-3/2	25792
7D-3/2	26048
7D-5/2	26069
9S-1/2	26911
5F	26971
9P-1/2	27637
9P-3/2	27682
8D-3/2	27811
8D-5/2	27823
10S-1/2	38300
6F	28329
10P-1/2	28727
10P-3/2	28754
9D-3/2	28829
9D-5/2	28836
11S-1/2	29130
7F	29148
11P-1/2	29404
11P-3/2	29421
10D-3/2	29469
10D-5/2	29473
12S-1/2	29666
8F	29679
12P-1/2	29853
12P-3/2	29865
11D-3/2	29897
11D-5/2	29900
9F	30042
10F	31406
13S-1/2	31406
14S-1/2	31406

Dimers

At the temperatures and pressures of the Rocketdyne experiments, about 1 percent of the Rb and Cs vapor exists in the form of dimers. Both of these dimers have absorption bands in the red. Generally, their spectra are quite complicated and consist of a number of diffuse, ill-defined bands. None of the features in our emission spectra could be unequivocably identified as being dimer emission.

Alkali Halides

Not very much is known about the spectroscopy of the alkali halides. Their dissociation energies are listed in Table 3 . Almost certainly, none of the alkali halides is electronically excited. The highly exothermic reactions of the alkali-metal:halogen systems should excite levels up to about v = 100. It may be possible to observe radiation from these vibrationally excited species, although this has not been done in our experiments.

PREVIOUS ALKALI-METAL ATOM LASERS

Several lasers have been built using electronically excited Cs as the lasing species (Ref. 5). One of these was based on the coincidence of the 3888 Å emission of helium with the 6S-1/2 - 8P-1/2 transition of atomic cesium. Boechner demonstrated in 1930 that cesium fluorescence could be excited by a helium discharge, and in 1957 Butayeva and Fabrikant used this technique in a search for population inversions in cesium. Results were inconclusive. Townes et al (Ref. 6) in 1961 performed a complex calculation and showed that a population inversion could be expected in the 8P-1/2 - 8S-1/2 transition at 7.18 microns

and, in the 8P-1/2 - 6D-3/2 transition, at 3.2 microns with sufficient pumping. Although their attempt at building a laser was not successful, they observed fluorescence from the 4F state, which lies 150 cm^{-1} above the 8P-1/2 state and was probably excited by collisions. A year later Rabinowitz, Jacobs, and Gould (Ref. 7) succeeded in operating an optically pumped cesium-vapor laser at 7.18 microns. This was the first gas laser using optical pumping.

Sorokin and Lankard (Ref. 8) have reported a cesium atom laser based on photodissociation of the Cs_2 dimer similar to the iodine photodissociation laser based on photodissociation of CF_3I or CH_3I. They found that when the Cs_2 band, having its origin at 7667 Å, was excited with 1 to 2 megawatts peak power from a dye laser, the dimer dissociated to give one cesium atom in the 6S ground state and another in the 7P state. Superradiant emission without mirrors with 1 to 2 kw peak intensity was observed on the 3.095-micron 7P-1/2 - 7S-1/2 transition. Likewise, excitation of Rb dimers in equilibrium with Rb vapor with 500-megawatt ruby laser pulses produced lasing on the 2.293-micron 6P-1/2 - 4D transition and on the 2.254 micron 6P-3/2 - 4D transition.

These experiments demonstrate that the transition probabilities for cesium and rubidium atoms are such that with sufficient pumping a population inversion and lasing can readily be obtained.

RECENT WORK

In the report on the results of the Discovery of New Lasers contract (Ref. 9), the past work on alkali metal-halogen reaction system was discussed in detail. Since then a number of important studies have been performed. Ham (Ref. 10), Hershbach (Ref. 11 and 12), and Zare (Ref. 13) have provided proof that direct excitation occurs by the

secondary reaction. Zare (Ref. 4) has studied in detail the chemiluminescent spectra of alkali-halogen reactions at low pressures (<1 mtorr). He shows that the reaction

$$M_2 + X_2 \longrightarrow MX^* + MX$$

can take place where MX* is the excited alkali halide. This reaction does not appear to be important at our pressures.

KINETICS OF POPULATION INVERSIONS

For the cesium-fluorine reaction system the largest population inversion was observed between the 5D and 6P states. For the purposes of these arguments we shall not consider the sublevels of these states. This approach is justified since the splitting of the sublevels is often 1 cm^{-1} or less meaning that only a few collisions are needed to thermally equilibrate their populations. The 5D state is pumped by radiative decay from higher levels and by external pumping by CsF(v). It radiatively decays only to the 6P state, which decays only to the 6S-1/2 ground state. At steady state, the flux into the 5D state is equal to the radiative flux out, $K_{5D}\ X_{5D}$, where X_{5D} is the state population and K_{5D} is the radiative rate constant. This in turn is equal to K_{6P} and X_{6P}, and thus

$$\frac{X_{5D}}{X_{6P}} = \frac{K_{6P}}{K_{5D}}$$

This approach ignores pumping of the 6P level, which would decrease the inversion, or collisional deactivation, which would maintain the ratio as long as it was not selective. Only selective deactivation of the 6P state could increase this ratio. Using the rate constantsof O. S. Heavens (Ref. 1), this ratio is calculated and shown in Table 7. The ratio for cesium is close to that observed, but for rubidium the observed ratio is about 1. This simple calculation shows that with suitable pumping, the radiative rate constants for all the alkali metals except lithium allow lasing on these

transitions. Their wavelengths shown in Table 7 are generally attractive. The cesium 3.6-micron transition lies in an atmospheric window.

TABLE 7. RATE RATIOS OF nD AND nP STATES FOR ALKALI METALS

ALKALI METAL	RATE RATIO	nD-3/2 ⟶ nP-1/2	nD-3/2 ⟶ nP-3/2	nD-5/2 ⟶ nP-3/2
Cs	34.2	3.010 microns	3.613	3.490
Rb	2.97	1.475	1.529	1.177
K	1.49	1.169	1.177	1.177
Na	1.19	0.818	0.819	0.819
Li	0.26	0.610	0.610	0.610

EXPERIMENTAL APPROACH

The fundamental approach of this work is to react alkali-metal vapor with a halogen, spectroscopically record the chemiluminescence, and to analyze it to find relative population inversions. The reaction occurs in a cavity exhausted by a 3000-cfm pump, and the chemiluminescence was observed through sapphire windows. A detailed description of the hardware, optical setup, and operational procedure has been presented in the report for the Discovery of New Lasers contract (Ref. 9). The hardware used in this work differs only in that a number of modifications were made. Nozzle modifications are described in the Nozzle Configuration Studies Section of this report.

One problem in the previous effort centered around thermal losses in the injector faceplate of the alkali-metal-halogen reactor. To reduce these losses, slots have been cut around the circumference of the injector faceplate to reduce thermal conduction to the flange, and the reactor shroud has been set off from the edge of the faceplate. Heat is brought to the faceplate assembly by hot nitrogen gas passed through a coil of tubing welded to the faceplate. Previously, this coil was made out of copper tubing that lost its mechanical properties at the high temperatures encountered. This copper tubing has been replaced by nickel tubing because of nickel's superior physical properties at high temperatures.

All the electrical heaters on the alkali-metal-halogen reactor have been replaced with new units. These heaters have been wired using ceramic-bead insulation because experience revealed that asbestos insulation does not retain its strength at the temperatures encountered. New thermocouples have also been installed. The reactor has been insulated with Cerafelt rock fiber insulation, which has superior mechanical properties to the Refrasil rock fiber insulation previously used.

New gas-heating ovens have been fabricated. These ovens are used to preheat gases before they enter the reactor and to heat the nitrogen gas used to heat the injector faceplate area and the baffle area of the reactor. Each oven is a 10-foot electrical heater wound with an equal length of stainless-steel tubing. Previously, each oven had a 250- or 500-watt capacity. The new ovens have a 1000-watt heating capacity and provide additional operating flexibility.

In this work, the capability to perform absorption experiments was added. A 750-watt quartz-iodine lamp was used as a light source because of its small filament size and increased output in the blue. To image the filament onto the flame, f/8 optics were used, giving an image size 1 mm x 3 mm.

EXPERIMENTAL RESULTS

In the experimental phase of this work relative state populations were determined for the Rb/Cl_2 system under fixed-point conditions. A parametric study was made on the Cs/F_2 system to determine the effect of initial reactant ratios and pressures. The spatial extent of an important population inversion was measured. A gain calculation was performed for the population inversions seen in the Cs/F_2 reaction system under optimum conditions. Studies were also performed on flame shape and the effect of different nozzle configurations.

FIXED-POINT STUDIES FOR Rb/Cl_2 SYSTEM

Of the four possible reaction systems with rubidium or cesium as the alkali metal and chlorine or fluorine as the halogen, the Rb/Cl_2 reaction system is the least promising on the basis of energetics (See Table 1). Because population inversions in the Cs/F_2 reaction system already had been demonstrated in the previous Discovery of New Lasers contract, it was decided to measure the populations of excited electronic states of the rubidium atom in the Rb/Cl_2 system as a worst-case situation. If inversions could be found in this system, then it would be likely that the other halogen-containing molecules such as ClF_3, ClF_5, and N_2F_2 would yield population inversions with cesium or rubidium as these reaction systems have low exothermicity also.

Spectra were obtained in the infrared and visible for the Rb/Cl_2 reaction system using the old nozzle configuration. Transitions were identified and their intensities were measured. From these intensities and the radiative transition probabilities published in the literature (Ref. 1 and 3), the relative population of each state corresponding to the upper level of an observed transition was calculated. These relative populations are shown in Table 8. The values used for the radiative transition probabilities were theoretical values, because experimental values do not exist for some of the transitions observed between the higher excited states. For the transitions

between lower states, including the ground state, the agreement between theory and experiment is fairly good. In cases where several observed transitions originated from one upper level, the relative population reported in Table 8 is an average value. The individual values are generally close to the average value.

The relative populations in Table 8 were obtained at a total pressure of 1 torr. The halogen gas stream was initially 1 torr Cl_2 and the alkali-metal-helium gas stream was initially 0.1 torr Rb plus 0.9 torr helium carrier gas for a 10:1 halogen-alkali-metal reactant ratio. The pressures specified above for each gas stream are before mixing. Since nozzle flow is subsonic, the mole flowrates primarily determine flame shape. The total cavity pressure is primarily determined by the helium gas window purge and the helium gas base bleed. Initial reactant gas temperature was 300 C.

The population inversions and their wavelengths are listed in Table 9. Inversions were measured with transition wavelengths from 1.1 to 28.9 microns. Table 10 shows rates of pumping of each state by an external source (probably in this case the RbCl(v) molecule). The pumping rate is calculated for each state by subtracting the amount exiting to other lower states from the amounts entering from other higher states. These relative pumping rates are calculated with a computer program that uses the radiative transition probabilities between states and the relative populations in Table 9. The pumping rate for the 5D-3/2 state is negative. Since this state is long lived, this negative number is interpreted to be the result of collisional quenching which, in effect, is negative pumping. The numbers in Table 10 indicate that pumping is not preferentially into any one state or even into the higher states collectively. Pumping seems to decrease with increasing state energy as if the pumping rate depended upon the energy distribution in the vibrationally excited RbCl. If the vibrational distribution were Boltzman or quasi-Boltzman, the pumping rate distribution might be explained. Also, the pumping rate distribution and thus the population distribution seem to

TABLE 8. RELATIVE POPULATIONS FOR Rb/Cl_2 REACTION SYSTEM

STATE	POPULATION
6S-1/2	25
5P-1/2	100
5P-3/2	81
6P-1/2	14
6P-3/2	14
7P-1/2	43
7P-3/2	17
4D-3/2	37
4D-5/2	87
5D-3/2	5.8
5D-5/2	11.
6D-3/2	1.4
6D-5/2	5.4
4F	5.8
5F	11
6F	8.0

TABLE 9. POPULATION INVERSIONS FOR Rb/Cl_2 REACTION SYSTEMS

UPPER STATE	POPULATION	LOWER STATE	POPULATION	TRANSITION WAVELENGTH
7P-1/2	43	4D-3/2	37	1.179 Microns
7P-1/2	43	6S-1/2	25	1.298
4D-5/2	87	5P-3/2	81.	1.529
6F	8.0	5D-3/2	5.8	2.029
7P-3/2	17	5D-3/2	5.8	4.609
7P-3/2	17	5D-5/2	11	4.615
7P-1/2	43	5D-3/2	5.8	5.684
7P-1/2	43	5D-5/2	11.	4.691
6F	8.0	6D-3/2	1.4	5.153
6F	8.0	6D-5/2	5.4	5.159
7P-3/2	17	7S-1/2	0	6.415
7P-1/2	42.8	7S-1/2	0	6.563
6F	8	5G	0	7.518
5F	11	6D-3/2	1.4	16.936
5F	11	6D-5/2	5.4	17.001
6F	8.0	7D-3/2	0	28.775
6F	8.0	7D-5/2	0	28.900

TABLE 10. EXCITATION INTO EACH EXCITED STATE

STATE	EXCITATION
6S-1/2	3.4×10^{8} sec^{-1}
5P-1/2	2.9×10^{9}
5P-3/2	1.5×10^{9}
6P-1/2	1.1×10^{8}
6P-3/2	1.0×10^{8}
7P-1/2	1.6×10^{8}
7P-3/2	6.9×10^{7}
4D-3/2	3.0×10^{8}
4D-5/2	9.1×10^{8}
5D-3/2	-3.8×10^{7}
5D-5/2	1.4×10^{7}
6D-3/2	4.1×10^{6}
6D-5/2	2.2×10^{7}
4F	8.3×10^{7}
5F	9.5×10^{7}
6F	4.1×10^{7}

indicate that states of high quantum number L (L(nF)=3,L(nD)=2, L(nP)=1, L(nS)=0)) are excited preferentially. Similar facts are found for the Cs/F_2 reaction systems. Because little is known about vibrational-to-electronic energy transfer, these facts are of great interest and further theoretical interpretation is underway at this time.

The Rb/Cl_2 reaction system does have the potential to lase despite the poor exothermicity (ΔH = -47 Kcal/mole for the primary reaction). Thus it is probable that reaction systems of cesium or rubidium with other halogen-containing molecules also have the potential for lasing as the low exothermicity of these reaction systems is not expected to be an obstacle.

FLAME SHAPE STUDIES

To study flame structure in detail, Cs/F_2 flames were photographed.

All these flames are at a total cavity pressure near 1 torr with a 1:1 reactant ratio. Only the reactant flowrates and the flowrates of the helium diluent gas have been varied. Total cavity pressure is determined by the pumping rate and by window purge and base-bleed flowrates.

The Cs/F_2 flame in Fig. 5 has reactant pressures of 1 torr cesium and 1 torr fluorine. Flowrates are such that the flame is contracting. The conical nozzle insert is visible at the bottom of the flame. It lifts the flame about 0.3 inch off the nozzle assembly and the cesium-helium mixture exits through its center. The fluorine-helium mixture exits through 18 small nozzles on the upper face of the nozzle assembly. For this type flame the area of maximum gain is about 0.4 inch above the conical nozzle insert (0.5-inch diameter). The body of the flame is purple in color and its outer sheath is bluish. The blue part of the flame is actually a region of less excitation since some of the lower excited states emit in the blue.

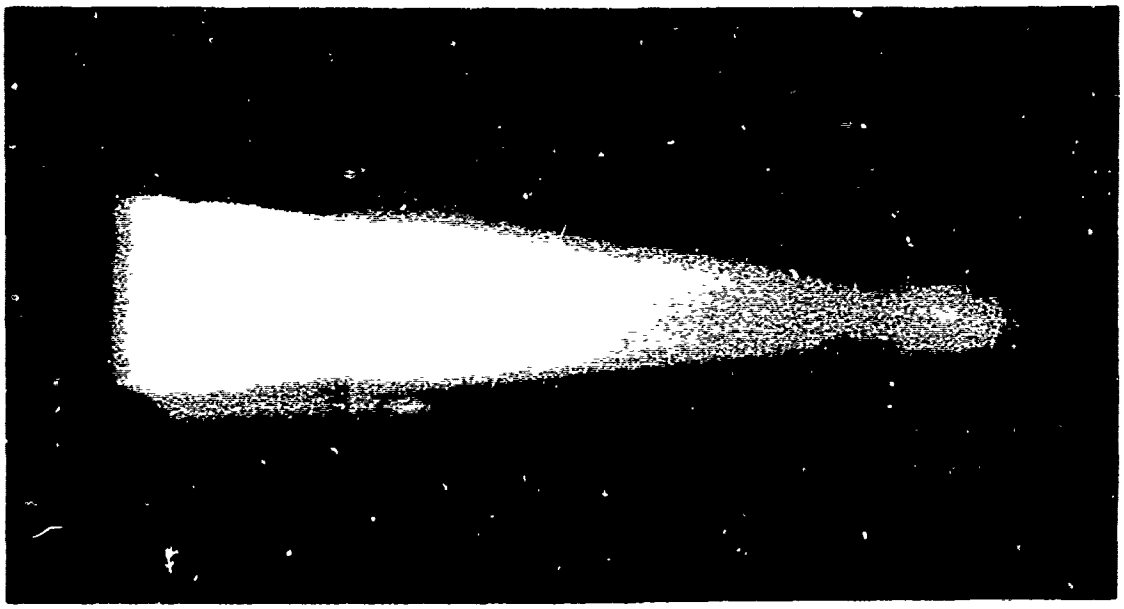

Figure 5. Cesium-Fluorine Flame

Figure 6 shows a high flowrate constant cross-section flame. The flame is purple like other Cs/F_2 flames. The structure on the edge of the flame is caused by droplets of cesium metal on the window caused by excess pressure during startup.

Figure 7 shows a flame with structure probably due to supersonic flow, the white area caused by overexposure of the purple part of the flame. The pinch at the center is caused by impingement of the surrounding fluorine flow.

Figure 8 shows a flame for low pumping rates and low flowrates. An inner core is visible. On the right edge of the nozzle some cesium metal is adhering to the outside of the conical nozzle insert while burning.

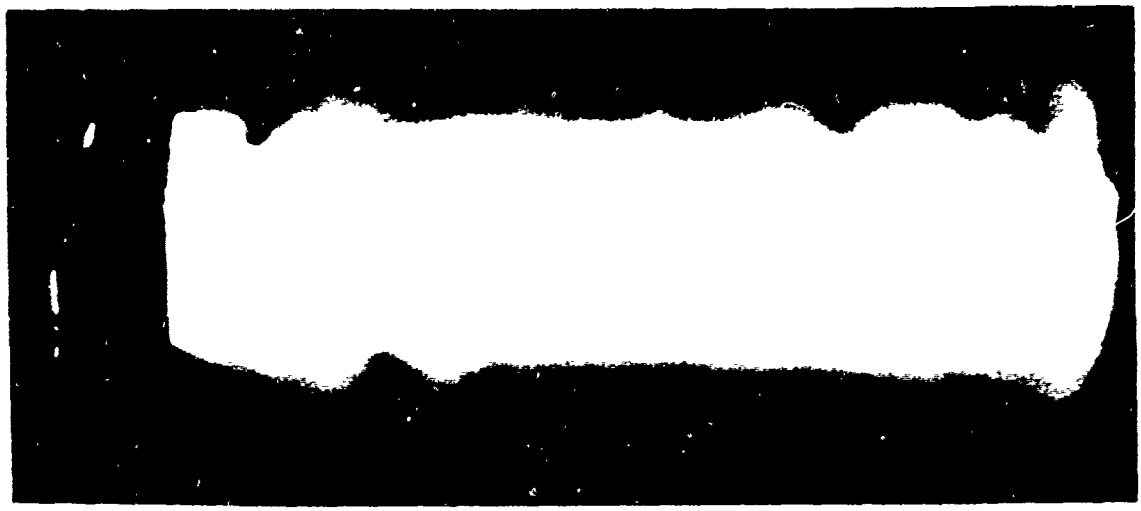

Figure 6. Cesium-Fluorine Flame

Figure 7. Cesium-Fluorine Flame

Figure 8. Cesium-Fluorine Flame

NOZZLE CONFIGURATION STUDIES

The nozzle on the alkali-metal-halogen reactor consists of 19 elements, each about 7 millimeters across. Each element consists of an outer annular slot for the halogen and an inner hole for the alkali-metal-helium mixture. In the previous work (Ref. 9) it was found that while this configuration gave very good mixing, the gas flows were eventually choked off by deposition of alkali halide on the nozzle assembly. Furthermore, the reaction area was larger than necessary for the chemiluminescence measurements, and thus the alkali-metal consumption rate was larger than necessary.

As part of the reactor modifications two types of plugs were machined. One type plugs the outer annular slot and the other type the inner hole. In the first nozzle configuration tried, only the center element of the nozzle assembly was left unplugged and the halogen and the alkali metal mixed within 1 or 2 millimeters of the nozzle assembly. With this configuration no combination of flowrates were found that prevented the deposition problem. Another configuration tried was the alkali-metal-helium mixture through the center element and halogen gas through the six elements immediately surrounding the center element. With this configuration the deposition decreased but mixing seemed slow, giving a diffused low-intensity flame. In the third configuration the alkali-metal-helium gas mixture came through the center nozzle element and the halogen through all the 18 remaining nozzle elements. In addition for the halogen elements the plugged center tubes were bent away from the center element, thus directing the halogen gas streams toward the alkali-metal-helium stream. Because these center tubes are nickel, they easily can be bent small amounts in any direction without risk of damage. This configuration eliminated the deposition problem and gave a reasonably bright flame with medium alkali-metal vapor flowrates. With high alkali-metal flowrates the deposition problem recurred. An insert was made for the center nozzle element. It is conical in shape and has a diameter of 0.5 inch at the exit. The alkali-metal-helium vapor exits through this

insert and the fluorine comes from the 18 elements surrounding it. The insert lifts the reaction flame off the nozzle assembly and increases the diameter of its base. This nozzle configuration eliminated the deposition problem and is visible in the photographs, e.g., Fig. 5.

REACTANT RATIO STUDIES

To study the effect of reactant ratios on the state populations of the Cs/F_2 reaction system, a test was performed in which the cesium-helium stream contained 0.1 torr Cs vapor plus 0.9 torr helium, and the fluorine stream was 1 torr F_2. Total pressure was 1 torr. This test was for the 10:1 fluorine-cesium ratio. In the next test the cesium-helium stream was unchanged, but helium was substituted for some fluorine in the outer stream to give 0.1 torr fluorine plus 0.9 torr helium, corresponding to a 1:1 reactant ratio. In the third test still more helium was substituted for fluorine to give for the outer stream 0.99 torr helium plus 0.01 torr fluorine, corresponding to a 0.1:1 reactant ratio. The substitution of helium buffer gas for fluorine ensured that total pressure, flame shape, and flame temperature were nearly the same for all three tests.

The reactant partial pressures above specify the partial pressure of the reactant before any mixing has occurred. For instance, 1 torr F_2 means that the fluorine-helium stream is 1 torr fluorine as the stream leaves the fluorine nozzles. In the flame photographs (Fig. 5 and 7), a bright outer shell is visible. As for these alkali-metal-halogen systems reaction occurs in about one collision, it is likely that most of the chemiluminescence is emitted from the shell region of the flame and that the reactants have nearly their initial partial pressure inside and outside of the shell region. However, as much of the chemiluminescence comes from the shell region, the observed reaction occurs at reactant partial pressures that vary widely in an unknown way. Then 1:1 reactant ratio must be understood as only a way of specifying one aspect of the flame and not as a statement of exact partial pressures in the reaction zone.

The spectroscopic data were reduced to state populations in the manner described previously (Ref. 9) using radiative rate constants published in the literature. The populations for all three reactant ratio tests are shown in Table 11. For all population tests the population of the 6P-1/2 is normalized to 100. For the 0.1:1 fluorine-cesium ratio only a few lines were observed. In part this is due to the low partial pressure of the limiting reactant (fluorine), which gave low chemiluminescence intensity, and in part it is due to the inability of this reactant ratio to produce satisfactory inversions. For instance, the 5D-3/2/6P-1/2 inversion is one-third of its value for the 1:1 reactant ratio.

On examining the data in Table 11, it is concluded that the 1:1 reactant ratio is best for producing population of the higher excited states of the Cs atom. An explanation for this is that an excess of F_2 relaxes the vibrationally excited CsF, whereas an excess of Cs collisionally quenches electronically excited Cs.

Table 12 lists the population inversions observed for the 10:1 reactant ratio and for the 1:1 reactant ratio. Inversions are seen from 1.9 microns to 77.5 microns. Some inversions are seen for the 10:1 reactant ratio that are not seen for the 1:1 reactant ratio. The explanation for this is that for the 10:1 reactant ratio case some of the higher D states are occupied, yet some of the higher P states are not, producing a population inversion. For the 1:1 reactant ratio case both are occupied. It is concluded that for lasing on certain transitions, some collisional deactivation is necessary. Another conclusion is that collisional deactivation may preferentially affect certain states (for instance, P states in preference to D states).

Table 13 shows the state pumping rates for the 10:1 and 1:1 reactant ratios. The rate for each state is the rate of pumping into that state by some external source. It is for each state S the flow of excitation to all lower states (from state S) minus the flow of excitation by decay from all higher

TABLE 11. STATE POPULATIONS AS A FUNCTION OF REACTANT RATIO (FLUORINE:CESIUM)

STATE	10:1 RATIO	1:1 RATIO	0.1:1 RATIO
7S-1/2	83	37.	--
8S-1/2	3.4	15.	--
9S-1/2	--	3.3	--
6P-1/2	100	100	100
6P-3/2	109	129	98
7P-1/2	21.	68.	--
7P-3/2	14.	25.	--
8P-1/2	2.7	12.	--
8P-3/2	2.7	6.5	--
9P-1/2	--	14.	--
9P-3/2	--	14.	--
5D-3/2	3900	3500	1000
5D-5/2	3900	3500	--
6D-3/2	5.8	18.	9.0
6D-5/2	5.2	8.7	9.0
7D-3/2	3.4	10.	9.4
7D-5/2	3.4	10.	9.4
8D-3/2	0.62	2.1	--
8D-5/2	1.1	2.9	--
4F	3.4	23.	--
5F	1.8	10.	--
6F	1.3	4.7	10.
7F	1.1	1.9	
8F	1.9	5.6	

TABLE 12. POPULATION INVERSIONS MEASURED IN RATIO STUDIES

			10:1 Ratio		1:1 Ratio	
UPPER STATE	LOWER STATE	TRANSITION WAVELENGTH	UPPER STATE POPULATIONS	LOWER STATE POPULATIONS	UPPER STATE POPULATIONS	LOWER STATE POPULATIONS
9P-3/2	6D-5/2	1.980			14.	8.7
9P-1/2	6D-5/2	1.988			14.	8.7
5F	6D-5/2	2.304			10.	8.7
5D-5/2	6P-1/2	2.924	4000	100	3500	100.
5D-3/2	6P-1/2	3.011	4000	100	3500	100.
7P-1/2	7S-1/2	3.095			68.	38.
8P-1/2	6D-5/2	3.249			12.	8.7
5D-5/2	6P-3/2	3.490	4000	109	3500	129.
5D-3/2	6P-3/2	3.614	4000	109	3500	129.
4F	6P-3/2	5.310			23.	18.
8F	8D-3/2	5.353	1.9	0.63	5.6	2.0
8F	8D-5/2	5.387	1.9	1.1	5.6	2.9
4F	6D-5/2	5.434			23.	8.7
9P-3/2	7D-3/2	6.119			14.1	10.
9P-3/2	7D-5/2	6.199			14.	10.
9P-1/2	7D-3/2	6.293			14.	110.
9P-1/2	7D-5/2	6.377			14.	10.
7F	8D-3/2	7.479			1.1	0.62
8F	9D-3/2	11.764	1.9	0.	5.6	0.
8F	9D-3/2	11.862	1.9	0.	5.6	0.
9P-3/2	9F-1/2	12.970			14.	3.3
9P-1/2	9S-1/2	13.774			14.	3.3
6F	8D-3/2	19.305	1.3	0.62	4.7	2.0
6F	8D-5/2	19.762	1.3	1.1	4.7	2.9
7D-3/2	8P-1/2	27.777	3.4	2.7	4.7	2.9
7D-3/2	8P-1/2	29.498	3.4	2.7	4.7	2.9
7F	9D-3/2	31.348	1.1	0	1.9	0
7F	9D-5/2	32.051	1.1	0	1.9	0

TABLE 12. (Concluded)

UPPER STATE	LOWER STATE	TRANSITION WAVELENGTH	10:1 Ratio		1:1 Ratio	
			UPPER STATE POPULATIONS	LOWER STATE POPULATIONS	UPPER STATE POPULATIONS	LOWER STATE POPULATIONS
7D-5/2	8P-3/2	36.101	3.4	2.7	10.	6.5
7D-3/2	8P-3/2	39.062	3.4	2.7	10.	6.5
8F	10D-3/2	47.619			5.6	0
8F	10D-5/2	48.54			5.6	0
8F	10D-3/2	47.019	1.9	0.		
8F	10D-5/2	48.543	1.9	0.		
8D-5/2	9P-1/2	53.763	1.1	0.		
8D-3/2	9P-1/2	57.471	0.62	0.		
8D-5/2	9P-3/2	70.922	1.1	0.		
8D-3/2	9P-3/2	77.519	0.62	0.		

TABLE 13. PUMPING RATES AS A FUNCTION OF REACTANT RATIO (FLUORINE:CESIUM)

STATE	RATES FOR 10:1 RATIO	RATES FOR 1:1 RATIO
7S-1/2	1.4×10^{9} sec^{-1}	3.3×10^{8} sec^{-1}
8S-1/2	3.2×10^{7}	1.4×10^{8}
9S-1/2	- - -	1.4x107
6P-1/2	-1.0×10^{9}	-4.9×10^{8}
6P- /2	-5.5×10^{8}	9.7×10^{8}
7P-1/	1.0×10^{9}	3.4×10^{9}
7P-3/2	1.3×10^{9}	2.4×10^{9}
8P-1 2	1.5×10^{8}	6.5×10^{8}
8P-3/2	2.9×10^{8}	7.0×10^{8}
9P-1/2	- - -	6.1×10^{8}
9P-3/2	- - -	1.2×10^{9}
5D-3/2	2.9×10^{9}	-3.2×10^{8}
5D-5/2	1.7×10^{9}	-3.1×10^{8}
6D-3/2	-3.6×10^{7}	-5.3×10^{8}
6D-5/2	-1.0×10^{8}	-7.7×10^{8}
7D-3/2	3.4×10^{7}	-2.0×10^{8}
7D-5/2	3.6×10^{7}	-3.6×10^{8}
8D-3/2	3.9×10^{6}	1.2×10^{7}
8D-5/2	7.6×10^{6}	1.8×10^{7}
4F	8.4×10^{7}	5.8×10^{8}
5F	2.4×10^{7}	1.3×10^{8}
6F	9.9×10^{6}	3.5×10^{7}
7F	5.0×10^{6}	8.7×10^{6}
8F	5.49×10^{6}	1.6×10^{7}

populated states (to state S). The negative rates correspond to collisional quenching of the excited state or of other excited states that drain into that excited state. The lower D states are longer lived and are thus more likely to be deactivated collisionally. Also, for the 1:1 reactant ratio the higher states are more populated than for the 10:1 reactant ratio. In Fig. 9 a visible spectrum of the chemiluminescence for Cs/F_2 is shown for this ratio. More than two dozen atomic cesium transitions are observed. Transitions of potassium and rubidium present as impurities are also seen.

As for the Rb/Cl_2 system, it is observed that for the Cs/F_2 system the pumping rate into each state decreases with increasing state energy. Furthermore, states with high quantum number L (such as the F states) seem to be preferentially pumped over states with low quantum number L (such as the S states).

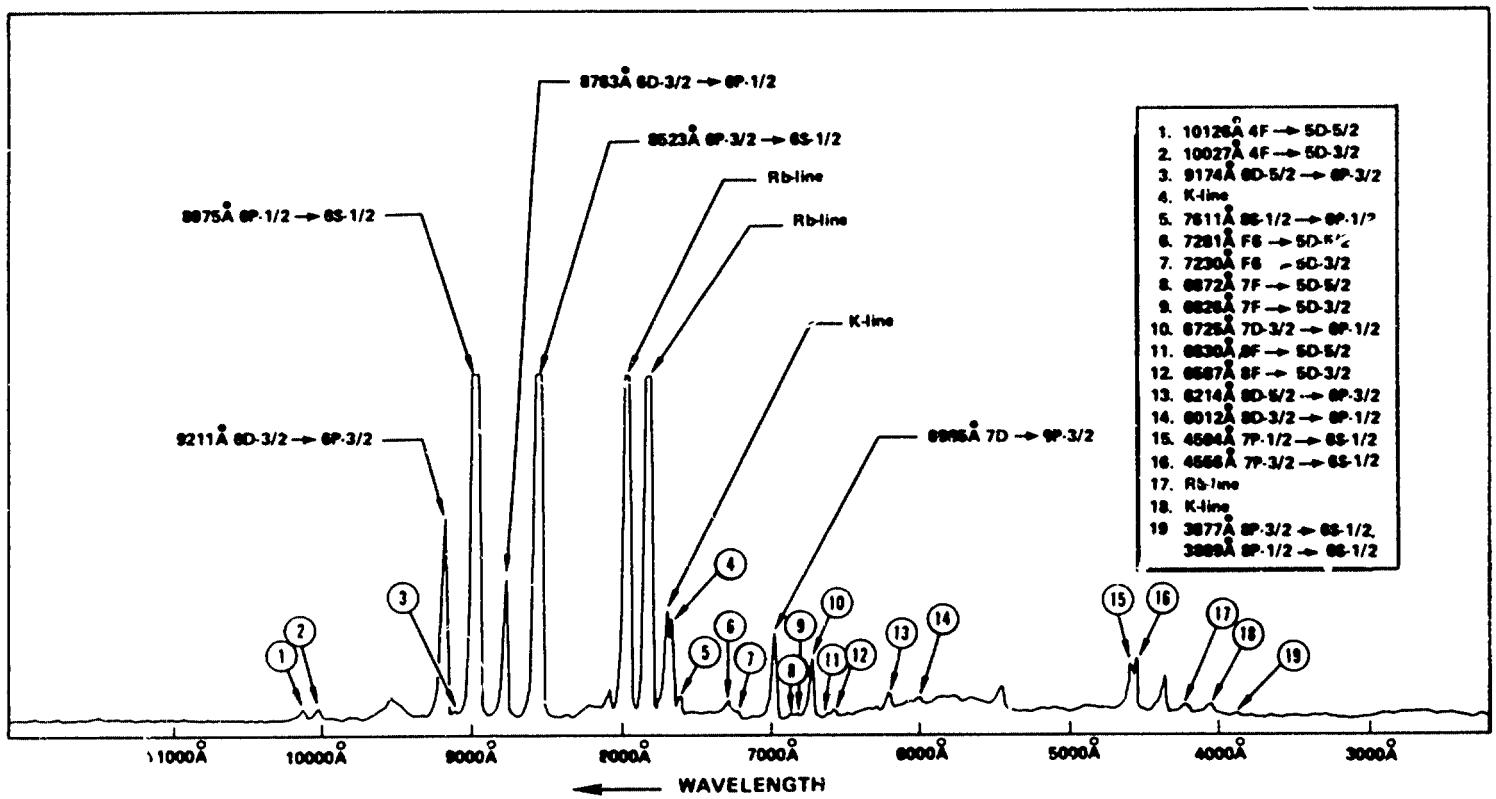

Figure 9. Visible Spectrum of the Chemiluminescence of the Cs/F_2 Reaction System

SPATIAL STUDIES

Three test runs were performed to determine the spatial distribution of an important population inversion as a function of distance downstream of the nozzle. For all tests total pressure was 1 torr. The helium-cesium gas mixture was 0.1 torr cesium plus 0.9 torr helium. The fluorine-helium gas flow was 0.9 torr helium plus 0.1 torr fluorine. The flowrate of the fluorine-helium stream for the first test run was about 3 times that of the cesium-helium stream producing a pointed flame like Fig. 5. In the second test run the ratio was 6 times, producing a still more contracted flame, and in the third test run the ratio was 10 times, producing a very short pointed flame.

The optical bench of Position No. 2 of Rocketdyne's CWLL facility can be moved by motor several inches in a vertical direction. This capability was used to perform vertical spatial scans. For the spatial scans, two spectrometers were used. A 0.3-meter McPherson equipped with a liquid nitrogen-cooled InSb detector was used to monitor the 5D-3/2 → 6P-3/2 transition at 3.614 microns. The optics of both systems were set up so that the same point in the flame was examined for each. The resolution of the system is about 0.05 inch.

For the first test case with a 3-to-1 flowrate ratio, the intensities of both transitions and the population inversion is shown in Fig. 10. The population inversion is spread out over about 0.3 inch. The maximum is at about 0.4 inch. All previous studies were performed at the fixed distance of 3/8 inch above the nozzle. Thus previous measurements for this study were probably near the point of maximum inversion in the flame. The spatial distributions for the second test run with 6-to-1 flowrate are shown in Fig. 11. The 6P-3/2 state shows a population distribution with two broad peaks, but the population of the 5D-3/2 state is sharply peaked at a distance of 1 inch above the nozzle. The distributions for the 10-to-1 flowrate case are shown in Fig. 12. The distribution of the 6P-3/2 state still shows two broad

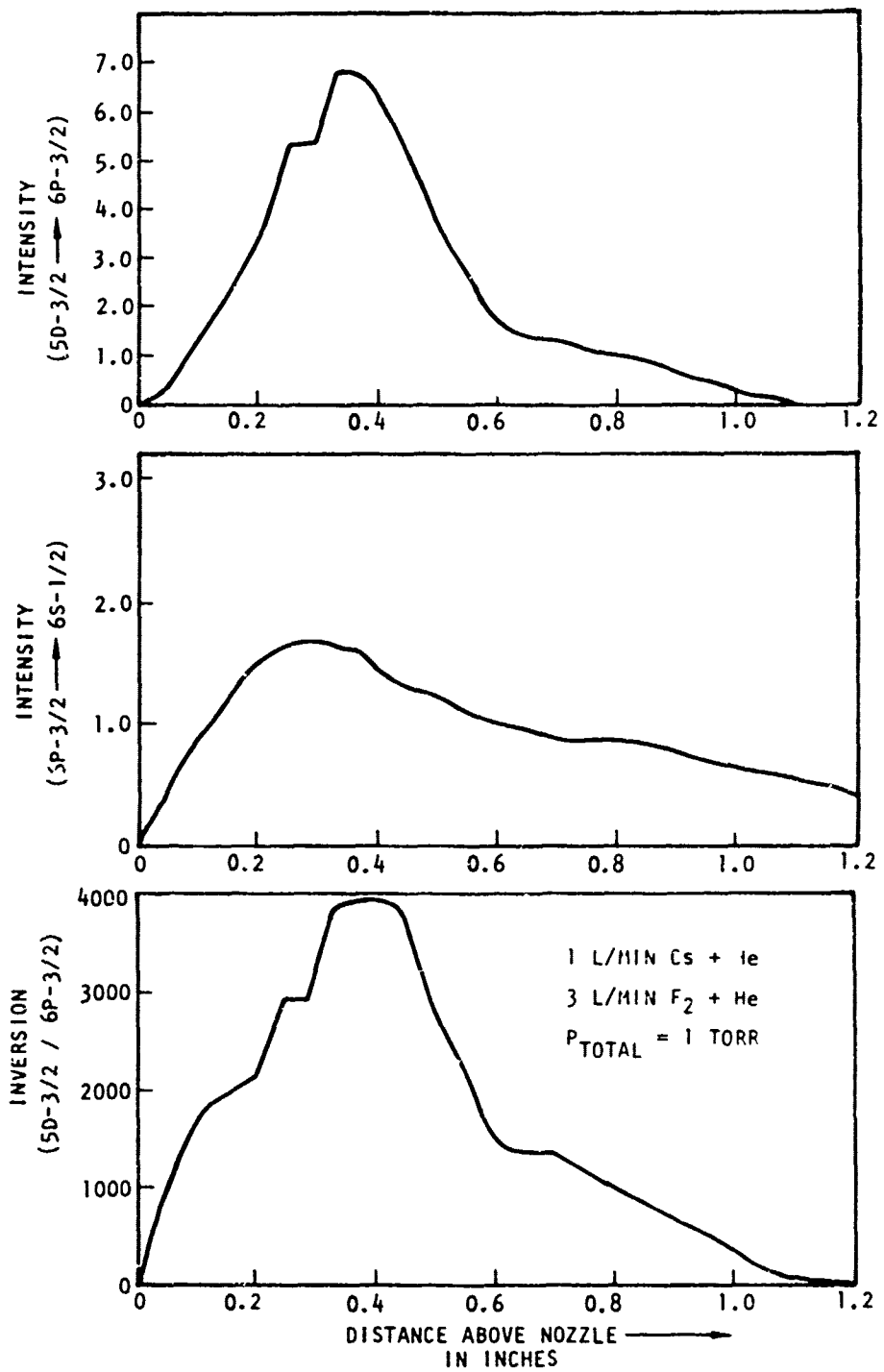

Figure 10. Spatial Distribution Line Intensities and Population Inversion in Cs/F_2 Flame

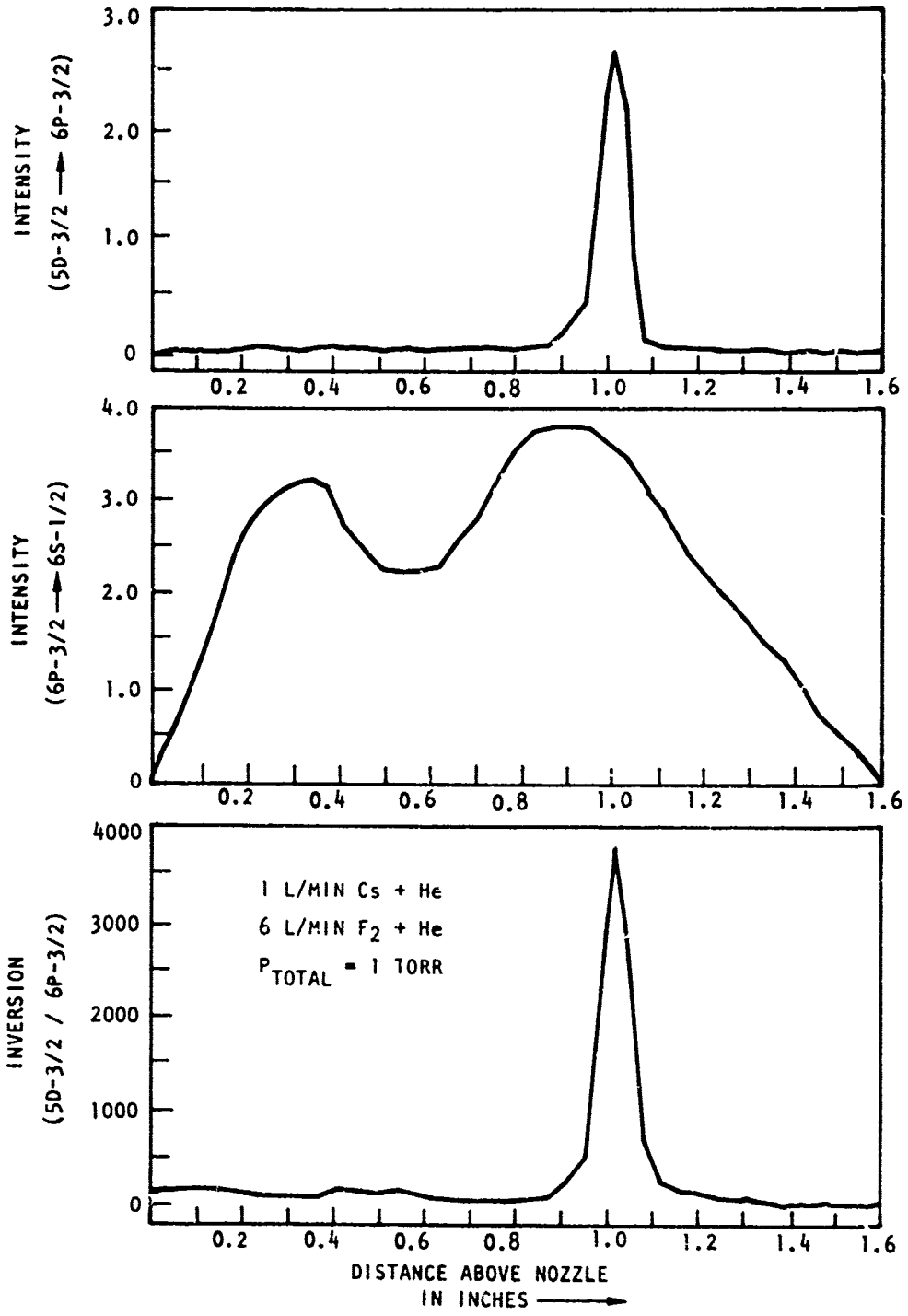

Figure 11. Spatial Distribution Line Intensities and Population Inversion in Cs/F_2 Flame

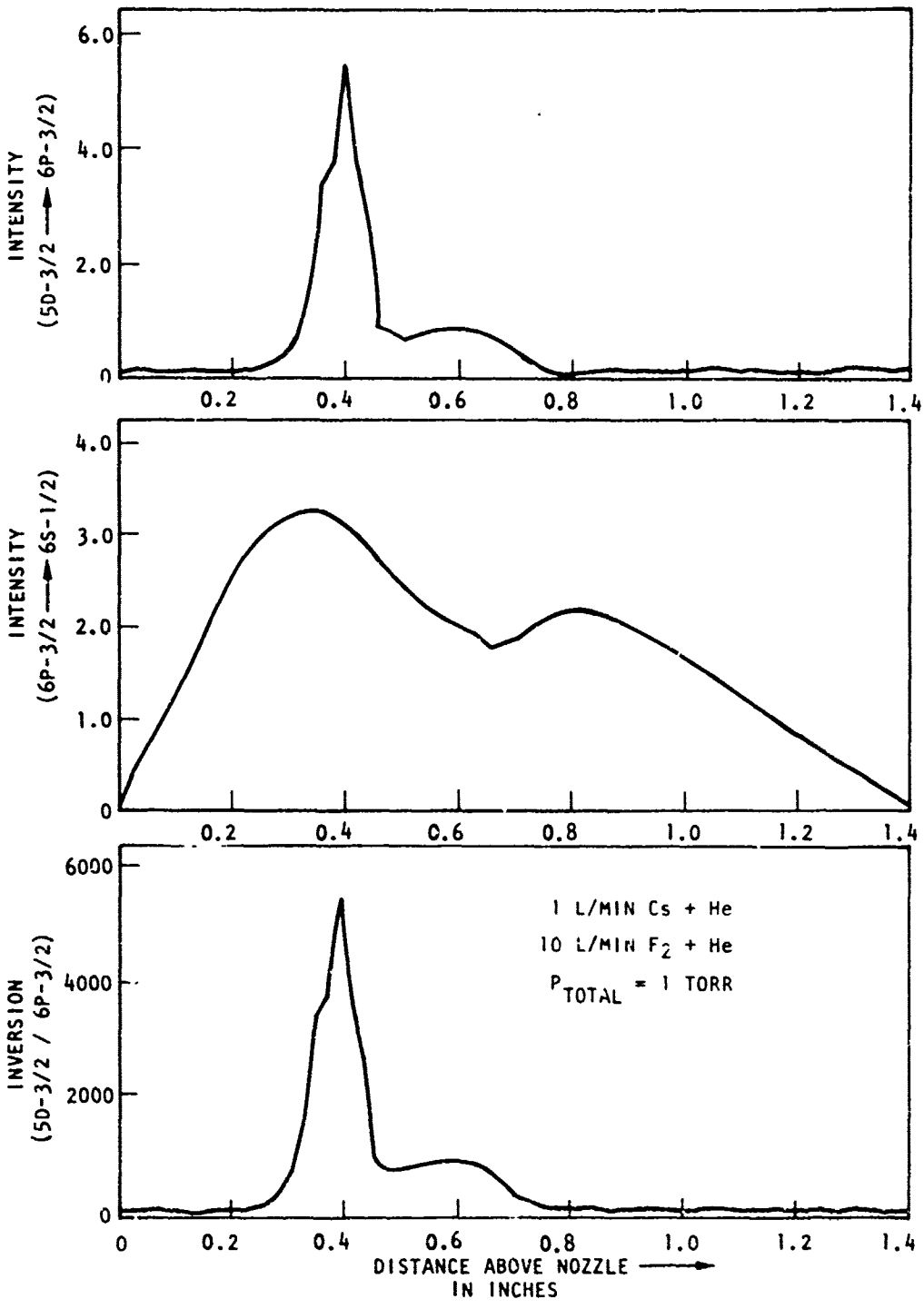

Figure 12. Spatial Distribution Line Intensities and Population Inversion in Cs/F_2 Flame

overlapping peaks, but the distribution of the 5D-3/2 state is now sharply peaked at about 0.4 inch above the nozzle.

With increasing fluorine flowrates the inversion has moved closer to the nozzle. These results indicate that for lasing a contracting sharply pointed flame should be avoided since the population inversion would be too localized. For a resonator configuration with a narrow beam waist, it might be difficult to align the optical system with the high gain region of the flame. With a wider gain region as in the first test case, this problem would be eliminated.

PRESSURE STUDIES

Two test runs were performed to give information on the pressure dependence of the population inversions observed in the cesium-fluorine reaction system. For test No. 1, the total cavity pressure was 16 torr. The fluorine-helium stream gas mixture was 8 torr fluorine plus 8 torr helium. The cesium-helium gas stream was 8 torr cesium vapor plus 8 torr helium gas. The 8-torr cesium vapor pressure was obtained by heating the cesium reservoir to 360 C. The high cavity pressure was obtained by throttling back the pumping system from its maximum capacity of 2600 cfm to about 400 cfm. At the necessary flowrates, the 8 ounces of cesium metal in the reservoir provided about 20 minutes of running time. The flame for test No. 1 was an expanding flame as pictured in Fig. 4. Its total length was 2 to 3 cm and it had a bluish tinge.

Test No. 2 was performed at a total pressure of 10 torr with the fluorine-helium stream 5 torr fluorine plus 5 torr helium. The cesium stream was 5 torr cesium plus 5 torr helium. The flame was a constant cross-section flame as in Fig. 2. The flowrates for test No. 2 were greater than in test No. 1 giving a longer flame.

In Table 14, the relative populations for these two pressure studies are shown. As before, the population of the 6P-1/2 state has been normalized to 100. Comparing these results with those in Table 11 for 0.1 torr cesium pressure, we notice that for these pressure tests the populations of the 7P and 8P states are lower considerably, but the populations of the 6D and 4F states are considerably higher. In Table 15 are the population inversions measured in these pressure tests. Inversions were observed for transitions from 1.6 to 77.5 microns. Some inversions are seen at these pressures (16 torr and 10 torr total pressure) that are not seen at lower pressures, and some inversions are not seen. The large inversions between the 5D and the 6P states remain. In test No. 2, they are significantly larger than those seen at lower pressures.

In Table 16 are the state pumping rates for these pressure studies. This rate is the rate of external pumping for each individual state. As before, the rates decrease with increasing energy, and for states of equal energy they seem to be greater for states with large quantum number L. There is a negative pumping rate into the 6P states which is probably due to the collisional deactivation. But the pumping rate of the 4F state (1.2×10^9 for pressure test No. 2) is greater than for the 4F state pumping rate for the 1:1 reactant ratio test (5.8×10^8) in Table 13 and much greater than for the 4F state pumping rate for the 10:1 reactant ratio test (8.4×10^7).

If the pumping mechanism is the primary reaction

$$Cs + F_2 \rightarrow CsF(v) + F$$

followed by a V-E transfer

$$CsF(v) + Cs \rightarrow CsF + Cs^*$$

TABLE 14. RELATIVE POPULATIONS FOR PRESSURE STUDIES IN Cs/F_2 REACTION SYSTEM

STATE	TEST NO. 1 16 TORR TOTAL PRESSURE	TEST NO. 2 10 TORR TOTAL PRESSURE
7S-1/2	83	82.
8S-1/2	12.	7.4
9S-1/2	1.6	--
6P-1/2	100.	100.
6P-3/2	97	139
7P-1/2	2.5	1.3
7P-3/2	2.5	8.5
8P-1/2	--	5.7
8P-3/2	--	5.7
5D-3/2	4000.	7200.
5D-5/2	4000.	4700.
6D-3/2	40.	31.
6D-5/2	41.	36.
7D-3/2	4.6	3.8
7D-5/2	6.6	4.2
8D-3/2	1.6	1.0
8D-5/2	3.0	1.0
4F	41.	51.
5F	22.	6.5
6F	3.7	1.9
7F	2.8	0.37
8F	--	1.9

TABLE 15. POPULATION INVERSIONS MEASURED IN PRESSURE STUDIES

UPPER STATE	LOWER STATE	TRANSITION WAVELENGTH, MICRONS	TEST NO. 1 16 TORR TOTAL PRESSURE		TEST NO. 2 10 TORR TOTAL PRESSURE	
			UPPER STATE POP.	LOWER STATE POP.	UPPER STATE POP.	LOWER STATE POP.
8D-5/2	7P-1/2	1.650	3.0	2.5	--	--
8D-5/2	7P-3/2	1.701	3.0	2.5	--	--
7D-5/2	7P-1/2	2.323	6.6	2.5	4.2	1.3
7D-3/2	7P-1/2	2.335	--	--	3.8	1.3
7D-5/2	7P-3/2	2.426	6.6	2.5	--	--
5D-5/2	6P-1/2	2.924	4000.	100.	4700.	100.
5D-3/2	6P-1/2	3.011	4000.	100.	7200.	100.
5D-5/2	6P-3/2	3.490	4000.	97.	4700.	139.
5D-3/2	6P-3/2	3.614	4000.	97.	7200.	139.
8S-1/2	7P-1/2	3.920	12.	2.5	7.4	1.3
8S-1/2	7P-3/2	4.219	12.	2.5	--	--
8D-5/2	8P-1/2	4.730	3.	0.	--	--
8D-3/2	8P-1/2	4.757	1.6	0.	--	--
8D-5/2	8P-3/2	4.923	3.0	0.	--	--
8D-3/2	8P-3/2	4.952	1.6	0.	--	--
4F	6D-3/2	5.310	41.	40.	51.	31.
8F	8D-3/2	5.353	--	--	1.9	1.0
8F	8D-5/2	5.387	--	--	1.9	1.0
7F	8D-3/2	7.479	2.8	1.6	51.	36.
9S-1/2	8P-1/2	8.319	1.6	0.	--	--
9S-1/2	8P-1/2	8.936	1.6	0.	--	--
5F	7D-3/2	10.834	22.	4.6	6.5	3.8
5F	7D-5/2	11.086	22.	6.6	6.5	4.2
6D-5/2	7P-1/2	11.547	41.	2.5	36.	1.3
8F	9D-3/2	11.764	--	--	1.9	0.
8F	9D-5/2	11.862	--	--	1.9	0.
6D-3/2	7P-1/2	12.150	40.	2.5	31.	1.3
6D-5/2	7P-1/2	14.598	41.	2.5	36.	8.5
6D-3/2	7P-3/2	15.576	40.	2.5	31.	8.5

TABLE 15. (Concluded)

UPPER STATE	LOWER STATE	TRANSITION WAVELENGTH, MICRONS	TEST NO. 1 16 TORR TOTAL PRESSURE		TEST NO. 2 10 TORR TOTAL PRESSURE	
			UPPER STATE POP.	LOWER STATE POP.	UPPER STATE POP.	LOWER STATE POP.
6F	8D-3/2	19.305	3.7	1.6	1.9	1.0
6F	8D-5/2	19.762	3.7	3.0	1.9	1.0
7D-5/2	8P-1/2	27.777	6.6	0.	--	--
7D-3/2	8P-1/2	29.498	4.6	0.	--	--
7F	9D-3/2	31.348	2.8	0.	0.37	0.
7F	9D-5/2	32.051	2.8	0.	0.37	0.
7D-5/2	8P-3/2	36.101	6.6	0.	--	--
7D-3/2	8P-3/2	39.062	4.6	0.	--	--
8F	10D-3/2	47.619	--	--	1.9	0.
8F	10D-5/2	48.543	--	--	1.9	0.
8D-5/2	9P-1/2	53.763	3.0	0.	1.0	0.
8D-3/2	9P-1/2	57.471	1.6	0.	1.0	0.
8D-5/2	9P-1/2	70.922	3.0	0.	1.0	0.
8D-3/2	9P-3/2	77.519	1.6	0.	1.0	0.

TABLE 16. STATE PUMPING RATES FOR PRESSURE STUDIES

STATE	TEST NO. 1 16 TORR TOTAL PRESSURE	TEST NO. 2 10 TORR TOTAL PRESSURE
7S-1/2	1.5×10^{9}	1.5×10^{9}
8S-1/2	1.2×10^{8}	7.0×10^{7}
9S-1/2	9.4×10^{6}	- - - -
6P-1/2	-1.5×10^{9}	-4.2×10^{9}
6P-3/2	-1.8×10^{9}	-9.1×10^{8}
7P-1/2	9.8×10^{7}	4.7×10^{7}
7P-3/2	1.8×10^{8}	7.9×10^{8}
8P-1/2	- - - -	3.1×10^{8}
8P-3/2	- - - -	6.1×10^{8}
5D-3/2	3.4×10^{9}	6.6×10^{9}
5D-5/2	2.0×10^{9}	1.8×10^{9}
6D-3/2	6.0×10^{8}	1.8×10^{8}
6D-5/2	6.5×10^{8}	1.5×10^{8}
7D-3/2	4.0×10^{7}	3.7×10^{7}
7D-5/2	6.1×10^{7}	6.2×10^{6}
8D-3/2	1.0×10^{7}	6.2×10^{6}
8D-5/2	1.9×10^{7}	6.2×10^{6}
4F	1.0×10^{9}	1.2×10^{9}
5F	2.9×10^{8}	8.5×10^{7}
6F	2.7×10^{7}	1.4×10^{7}
7F	1.3×10^{7}	1.6×10^{6}
8F	- - - -	5.4×10^{6}

with a quenching reaction

$$CsF(v) + F_2 \rightarrow CsF + F_2$$

the vibrational energy distribution of the CsF(v) and thus the electronic state distribution of the Cs* should not depend on reactant partial pressure as long as the reactant ratio stays constant. Although the rate of pumping varies with pressure, the ratio of the pumping rate (V → E) of the cesium atoms to the rate of deactivation (V → T, R and V → V) of CsF(v) should go as $[Cs]/[F_2]$, which is constant for our comparison. One possible explanation is that at higher reactant pressures a two-step pumping process becomes important:

$$CsF(v) + Cs(6S\text{-}1/2) \rightarrow CsF + Cs(6P)$$

$$CsF(v) + Cs(6P) \rightarrow CsF + Cs(6D,4F).$$

Such a two-step process could explain the observed state populations, the negative pumping rate into the 6P states, and the larger pumping rate into the 4F state at higher reactant pressures.

We conclude on the basis of these pressure studies that a large number of population inversions can be maintained at high reactant pressures and that the large population inversion between the 5D and 6P states is not decreased. Some population inversions are actually increased by the higher reactant pressures. While the maximum cesium pressure studied was 8 torr, it is reasonable to expect that the population inversions could be maintained at much higher pressures (perhaps several hundred torr). The reason for this is for these systems the fastest deactivation process is radiative deactivation between the electronic states of the cesium atom.

The 5D state is one of the longest-lived states with a lifetime of about 1 microsecond. Yet the configuration of radiative rate constants is such that large inversions can be maintained with large gain (see Gain Calculations section following). Only at higher reactant pressures would collisional quenching become more important than radiative deactivation.

Our maximum pressure of 8 torr cesium (360 C reservoir temperature) was limited by the mechanical properties of the all-metal stainless-steel welded Varian valves, which have a maximum operating temperature of 450 C. An attempt was made to run the valve at 375 C when a weld failure occurred releasing cesium metal into the reactor shroud. A search of the literature revealed that stainless steel is known to lose more than half of its mechanical strength when exposed to cesium (Ref. 15 and 16).

GAIN CALCULATIONS

Having established the presence of population inversions in the cesium-fluorine system, the next problem is to determine gain coefficient α as defined by the equation

$$I = I_o e^{\alpha x}$$

where X is the gain path length. The gain equation is (Ref. 17).

$$\alpha(\nu) = \left(N_2 - N_1 \frac{g_2}{g_1}\right) \frac{c^2}{8\pi \nu^2} \; A \; h(\nu - \nu_o)$$

where N_2 is the population of the upper state, the g's are the state degeneracies, ν is the transition frequency, A is the Einstein coefficient, and $h(\nu - \nu_o)$ is the lineshape function. An unsuccessful attempt (see next section) was made to measure the population of the excited 5D states by absorption spectroscopy. If this population were determined, the absolute population of all the excited states would be known.

However, the population of the 5D states can be estimated. For the sodium-chlorine reaction system, the measured quantum yield is 0.8 (Ref. 18). Because all the alkali-metal-halogen reaction systems are quite similar with nearly identical reaction rate constants, this value can be used as the quantum yield for the cesium-fluorine system. As this quantum yield was measured in the visible, more than 99 percent of the radiation detected came from the 6P and 6D states. Using the radiative flux between states calculated from the relative populations, this corresponds to a quantum yield of 0.58 for the 5D states and 0.34 for the 5D-3/2 state. For 1 torr cesium vapor at 300 C, this corresponds to a total density of 5D-3/2 states created of 5.7×10^{15} states/cc. However, the 5D-3/2 state decays with a lifetime of about 1 microsecond, meaning that only a small fraction of the total created is in existence at any one time. In our experiments, the reaction flame is about 2 cm in length and the flow velocity is about 2×10^4 cm/sec, corresponding to a flame dwell time of 100 microseconds. Assuming a uniform pumping region, 1 percent of the 5D-3/2 state created is in existence at any one time, corresponding to a state density

$$N_{5D\text{-}3/2} = 5.7 \times 10^{13} \text{ states/cc}$$

If the pumping region were shorter, the number density would be proportionately larger.

Using this number density and the relative populations for the 1:1 reactant ratio (Table 11), the gains have been calculated for the observed population inversions. A simple rectangular lineshape function was used with line width based on the line widths in the literature for the lower excited states (Ref. 19). The results are shown in Table 17.

Some of the inversions exhibit negative gain when the degeneracy factors are applied in the gain equation, and they are omitted from Table 17. For other inversions (9P-1/2 → 6D-5/2, for example) the radiative rate constant is

TABLE 17. CALCULATED GAINS FOR INVERSIONS IN Cs/F_2 REACTION SYSTEM

UPPER STATE	LOWER STATE	TRANSITION WAVELENGTH	GAIN α	X FOR SINGLE-PASS GAIN OF 6%
9P-3/2	6D-5/2	1.980 Microns	0.087 cm^{-1}	0.67 cm
9P-1/2	6D-5/2	1.998	--	--
5D-5/2	6P-1/2	2.924	--	--
5D-3/2	6P-1/2	3.011	5.6	0.011
7P-1/2	7S-1/2	3.095	0.23	0.25
8P-1/2	6D-5/2	3.249	--	--
5D-5/2	6P-3/2	3.490	7.8	0.0074
5D-3/2	6P-3/2	3.614	1.3	0.044
8F	8D-3/2	5.353	0.00016	360.
8F	8D-5/2	5.387	0.00018	329.
4F	6D-5/2	5.434	0.30	0.19
9P-3/2	7D-3/2	6.119	0.38	0.15
9P-3/2	7D-5/2	6.199	7.95	0.0073
9P-1/2	7D-3/2	6.293	5.85	0.0099
9P-1/2	7D-5/2	6.377	--	--
8F	9D-3/2	11.764	0.0019	29.
8F	9D-5/2	11.862	0.0032	18.
9P-3/2	9S-1/2	12.970	1.72	0.044
9P-1/2	9S-1/2	13.774	0.95	0.061
6F	8D-3/2	19.305	0.66	0.088
6F	8D-5/2	19.762	0.59	0.098
7F	9D-3/2	31.348	2.4	0.024
7F	9D-5/2	32.051	4.1	0.014
7D-5/2	8P-3/2	36.101	0.49	0.12
7D-3/2	8P-3/2	39.062	0.74	0.078
8F	10D-3/2	47.619	19.	0.0031
8F	10D-5/2	48.543	31.	0.0018

unknown since the transition is forbidden by the $\Delta J = 0, \pm 1$ selection rule. The radiative rate constant may be 2 to 4 orders of magnitude smaller than for allowed transitions in the same multiplet. However, it still might be possible to lase on these weak transitions using a frequency-selective resonator. In fact, the smaller radiative rate constant might be useful in preventing superradiancy and parasitic problems. Some of the transitions in Table 17 show so much gain that superradiancy may be a problem forcing operation with short lasing pathlengths.

Using the quantum yield of 0.58 calculated above for the 5D states and the exothermicity of the primary reaction (-85 Kcal/mole), we find that 11 percent of the reaction exothermicity is emitted in the 5D-6P transitions and should be available for lasing. It is remarkable that with all the electronic levels of the cesium atom that the radiative rate constants should be such that this fraction of the total energy flows through one inversion. The efficiency of this transition corresponds to 300 joules/gm Cs or 135 kjoules/lb cesium, 1050 joules/gm F_2 or 472 kjoules/lb F_2, or 233 joules/gm total or 104 kjoules/lb total. At our maximum flowrates of 8 ounces cesium in 15 minutes, 75 watts of energy are emitted by the 5D-6P transitions and theoretically would be available for lasing with the construction of an efficient resonator.

ABSORPTION/EXTINCTION STUDIES

An attempt was made to measure absorption from the 5D states to the higher P states. Based on the flame path length (1 cm), the number density of the 5D states (see previous section), and the radiative transition probabilities, the calculated absorptions were at the limits of detectibility (1 percent). If an absorption could be measured, it would give an experimental value for the population number densities of all the excited states. An attempt was made during test No. 2 of the pressure studies, but no absorptions were seen placing an upper limit on the number density for the 5D states (that of the

previous section). Due to the low sensitivity of the absorption method this unsuccessful attempt does not in any way indicate inadequate excited state number densities.

For initial reactant flowrates like those used in Ref. 14:

$$F_2 = 2.6 \times 10^{-3} \text{ moles/sec}$$

$$Cs = 2.6 \times 10^{-4} \text{ moles/sec}$$

$$He = 2.6 \times 10^{-4} \text{ moles/sec}$$

The exhaust consists of 2.6×10^{-4} moles/sec CsF in 2.8×10^{-3} moles/sec gas. The question arises as to what effect this amount of alkali halide has on the optical properties of the reaction gas mixture and a worst-case calculation is performed below in an attempt to answer it.

The cross section for extinction of a light beam by particulates is the sum of an absorption part and a scattering part,

$$C_{ext} = C_{scat} + C_{abs}$$

or if a dimensionless efficiency factor is defined as

$$Q = C/\pi a^2$$

where a is the particulate radius, then

$$Q_{ext} = Q_{scat} + Q_{abs}$$

It can be shown for particles of dimensions similar to that of the wavelength λ of the incident light (Ref. 20).

$$Q_{ext} = -Im\left\{4x\,\frac{m^2 - 1}{m^2 + 2} + \frac{4}{15}x^3\left(\frac{m^2 - 1}{m^2 + 2}\right)^2 \frac{m^4 + 27m^2 + 38}{2m^2 + 3}\right\} +$$

$$x^4 \; Re\left\{\frac{8}{3}\left(\frac{m^2 - 1}{m^2 + 2}\right)^2\right\} + \ldots$$

where m is the complex refractive index and $x = 2\pi a/\lambda$. Usually for small x the first term of this expression is sufficient. For an absorption coefficient, λ, defined in the usual manner,

$$I = I_o \varepsilon^{-\lambda d}$$

where d is the effective path length, then,

$$\lambda = C_{ext}\, N = \pi a^2\, Q_{ext}\, N$$

where N is the number of particles per unit volume of radius a.

For scattering (Ref. 20)

$$Q_{scat} = x^4\,\frac{8}{3}\left|\frac{m^2 - 1}{m^2 + 2}\right|^2 + \ldots$$

For a dielectric such as CsF, the imaginary part of the index of refraction is quite small and the extinction cross section is almost entirely due to scattering.

For the above alkali-metal-halogen flowrates, a particle concentration of 10^6 particles/cc is expected for a 0.5-micron particle diameter. Taking m= 1.64 for the index of refraction (Ref. 20), then at λ = 2 microns.

$$\lambda = 2 \times 10^{-4} \text{ cm}^{-1}$$

corresponding to a 0.7-percent loss for a 30-cm path length. For shorter λ, the loss would be greater. However, for $x \leq 1$, the above formula for scattering breaks down. The greatest extinction occurs when the particle diameter is equal to the wavelength. Thus, the number above is probably close to some maximum possible value.

Furthermore, for large x with large particle size with a fixed-mass flowrate, the total scattering cross section decreases with increasing particle size, as the total number of particles decreases as $1/r^3$, but the cross section per particle increases only as r^2.

In our experimental setup, reactant flow velocities of 10^4 cm/sec are expected, corresponding to a residence time of about 100 microseconds maximum in the reaction zone. For 0.1 torr of CsF molecules, this time corresponds to fewer than 100 CsF-CsF collisions. Thus, particulate diameter may be considerably less in the reaction zone than assumed in the above calculation. Scattering, likewise, would be smaller.

On the basis of these arguments extinction due to particulates would almost certainly be less than the value for λ above.

During test No. 2 of the pressure studies an attempt was made to measure extinction for the 1-cm pathlength at a frequency different from any of the cesium emission lines. None was seen meaning extinction is less than 1 percent/cm. This fact combined with the high gains observed means that CsF particulates should not be any obstacle to lasing.

CONCLUSIONS ABOUT OPTIMUM CONDITIONS FOR LASING

On the basis of this work, the optimum reactant ratio for lasing is 1:1 for the Cs/F_2 reaction system. Cesium reactant pressure can be varied for 8 to 0.1 torr without adversely affecting the large population inversions. However, some of the small population inversions are pressure-dependent. Extinction measurements show that scattering and absorption by the alkali-halide particulates will not be a problem.

Gain calculations show that there is more than enough gain for lasing on a number of transitions and, indeed superradiancy may be a problem. This could be alleviated by operating at low reactant pressures.

Nozzle configuration studies indicate that an impinging stream design is probably best for solving the problems of obtaining fast reactant mixing and at the same time preventing clogging of the nozzles by deposition of alkali-halides. Spatial studies showed that the region in the flame of optimum inversion is located about 0.4 inch from the nozzle assembly. At constant cavity pressure large reactant flowrates moved the inversion toward the nozzle assembly and narrowed its spatial distribution.

REFERENCES

1. Heavens, O. S.: "Radiative Transition Probabilities of the Lower Excited States of the Alkali Metals," J. O. S. A. 51, 1058-1061 (1961).

2. Kratz, H. R.: "The Principla Series of Potassium, Rubidium, and Cesium in Absorption," Phys. Rev. 75, 1844-1850 (1949).

3. Stone, M.: "Cesium Oscillator Strengths," Phys. Rev. 127, 1151-1156 (1962).

4. Anderson, E. M., and V. A. Zilities: "Semiempirical Calculation of Oscillator Strength for Lithium, Rubidium, and Cesium Atoms," Optics and Spectro. (USA) 16, 211-214 (1964).

5. Lengyel, B. A.: Introduction to Laser Physics, John Wiley and Sons, Inc., New York, p. 293 (1971).

6. Townes, C. H., et al.: "Alkali Vapor Infrared Masers," Advances in Quantum Electronics, Columbia University Press, New York, pp. 12-17 (1961).

7. Rabinowitz, P., S. Jacobs, and G. Gould: "Continuous Optically Pumped Cs Laser," Appl. Optics 1, pp. 513-516 (1962).

8. Sorokin, P. P., and J. R. Lankard: "Infrared Lasers Resulting From Photodissociation of Cs_2 and Rb_2," Journ. of Chem. Phys. 51, pp. 2929-2931 (1969).

9. Hall, L. H.: Discovery of New Lasers, Report RK-CR-73-5 (28 December 1973).

10. Ham, D. O.: Discuss. Faraday Soc. 55, p. 313 (1973).

11. Struve, W. S., T. Kitagawa, and D. R. Herschbach: J. Chem. Phys. 54, pp. 2759 (1971).

12. Struve, W. S., J. R. Krenos, D. L. McFadden, and D. R. Herschbach: Discuss. Faraday Soc. 55, pp. 314 (1973).

13. Oldenborg, R. C., J. L. Gole, and R. N. Zare: work described by P. J. Dagdigian, Discuss. Faraday Soc. 55, pp. 311 (1973).

14. Oldenborg, R. C., J. L. Gole, and N. Zare: Journ. Chem. Phys. 60, pp. 4032 (1974).

15. Klueh, R. L. and D. H. Jansen: Effects of Liquid and Vapor Cesium on Structural Materials, Report ORNL-TM-1813 (1967).

16. Stang, J. H., et al.: Compatibility of Liquid and Vapor Alkali Metals With Construction Materials, DMIC Report 227 (15 April 1966).

17. Yariv, A.: Quantum Electronics, John Wiley and Sons, Inc., New York (1968).

18. Magee, J. L.: "The Mechanism of Reactions Involving Excited Electronic States," Journ. of Chem. Phys. 8, pp. 687-698 (1940).

19. Chen, C. L. and A. V. Phelp: "Self-Broadening of Cesium Resonance Lines at 8521 and 8944 Å," Phys. Rev. 173, pp. 62 (1968).

20. Van deHulst, H. C.: Light Scattering by Small Particles, John Wiley & Sons, Inc., London (1957).